Internal Medicine
The Japanese Society of Internal Medicine
doi: 10.2169/internalmedicine.6717-20
Intern Med 60: 3809-3816, 2021
http://internmed.jp

【 CASE REPORT 】

Long Spinal Cord Lesions Caused by Venous Congestive Myelopathy Associated with Intravascular Large B-cell Lymphoma

Takeshi Miura[1], Shoji Saito[2,3], Rie Saito[2], Tomohiro Iwasaki[4], Naomi Mezaki[1], Tomoe Sato[1], Yoichi Ajioka[5], Akiyoshi Kakita[2] and Takuya Mashima[1]

Abstract:
Intravascular large B-cell lymphoma (IVLBCL) is a subtype of B-cell lymphoma, characterized by lymphoma cell proliferation within small blood vessels. We herein describe a rare case with long spinal cord lesions caused by venous congestive myelopathy associated with IVLBCL. An 81-year-old man presented with paraplegia of the lower limbs and sensory disturbances. Magnetic resonance imaging revealed intramedullary longitudinal T2-hyperintensity lesions in the thoracic cords. The patient died three months after disease onset, and a neuropathological analysis revealed predominantly atypical B-lymphocytes located sparsely in the veins of the spinal cord. IVLBCL should be considered in the differential diagnoses of long spinal cord lesions.

Key words: intravascular lymphoma, IVL, IVLBCL, MALT lymphoma, long spinal cord lesion, venous congestive myelopathy

(Intern Med 60: 3809-3816, 2021)
(DOI: 10.2169/internalmedicine.6717-20)

Introduction

Intravascular large B-cell lymphoma (IVLBCL) is a rare and distinct form of large B-cell lymphoma, characterized by the growth of malignant lymphocytes within the lumina of small blood vessels (1, 2). The growth of these lymphocytes may result in ischemic lesions, which can affect the spinal cord. However, few reports are available on long spinal cord lesions associated with IVLBCL; thus, the clinical features and pathomechanism underlying disease progression remain unclear. Therefore, when a patient shows long spinal cord lesions with predominantly neurological manifestations, it is challenging to identify IVLBCL as a cause of neurological symptoms. We herein investigated the clinicopathologic features of an autopsied case of an 81-year-old Japanese man presenting with long spinal cord lesions by venous congestive myelopathy associated with IVLBCL.

Case Report

A previously healthy 81-year-old Japanese man experienced dysuria two weeks before visiting our hospital, accompanied by sudden-onset hypoesthesia in his left lower limb, and the right lower limb soon thereafter. He also presented with muscle weakness of the lower limbs, which worsened rapidly and made standing difficult; thus, he was referred to our department and was hospitalized. On admission, he was alert, and the vital examination findings were as follows: body temperature, 36.8℃; arterial blood pressure, 99/40 (systolic/diastolic) mmHg; and pulse rate, 55/min.

Neurological testing revealed left-dominant incomplete paraplegia of the lower limbs. A manual muscle test (right/left) was performed to examine the gluteus maximus and iliopsoas muscles (2/1) and the quadriceps, hamstrings, tibialis anterior, and gastrocnemius muscles (1/0). Moreover, the

[1]Department of Neurology, Tsubame Rosai Hospital, Japan, [2]Department of Pathology, Brain Research Institute, Niigata University, Japan, [3]Department of Neurosurgery, Brain Research Institute, Niigata University, Japan, [4]Department of Internal Medicine, Tsubame Rosai Hospital, Japan and [5]Division of Molecular and Diagnostic Pathology Graduate School of Medical and Dental Sciences, Niigata University, Japan
Received: November 12, 2020; Accepted: May 7, 2021; Advance Publication by J-STAGE: June 19, 2021
Correspondence to Dr. Takeshi Miura, tmiura-nii@umin.ac.jp

Figure 1. **1.5 Tesla magnetic resonance imaging (MRI) of the spinal cord. a: On the first hospital day, T2-weighted image (T2WI, the left panel) shows an intramedullary lesion with high signal intensity at the T3 to T6 level. b: The second MRI 10 days after admission. T2WI hyperintensity lesions tend to expand and split between T3 to T4 and T5 to T6. c: The third MRI on the 18th day after admission. T2WI (the left panel) reveals that the hyperintensity lesions remain unchanged and gadolinium-enhanced T1WI (the right panel) demonstrates abnormal mild gadolinium enhancement on the dorsal edge of T4 to T5. d: The fourth MRI on the 44th day after admission. The T2WI (the left panel) shows that the hyperintensity lesions further expand and divide into the upper part of C7 to T4 and the lower part of T4 to T9. The gadolinium enhancement T1WI (the right panel) demonstrates the faint enhancement effect on the height of T4 to T5.**

patient exhibited hyperreflexia of the patellar and Achilles tendons, bilateral extensor plantar reflex, complete loss of superficial (touch, pain, and temperature) and vibration senses below the T10 level (defined by dermatome), and urinary retention. Spinal cord magnetic resonance imaging (MRI) revealed a hyperintensity lesion with cord swelling at the T3 to T6 level on T2-weighted images (T2WI, Fig. 1a) and diffusion-weighted images (data not shown). Subsequently, the lesion showed no improvement and extended from C7 to T9 on T2WI with mild gadolinium enhancement at T4 to T5 at the later disease stage (Fig. 1b-d). Laboratory findings (Table 1) indicated normocytic anemia, thrombocytopenia, and slightly elevated lactate dehydrogenase (LDH). There were no abnormal cells in a peripheral blood sample. The initial diagnosis was spinal cord infarction, and antiplatelet drugs were therefore administered; however, the patient's condition deteriorated rapidly and resulted in complete paraplegia of the lower limbs seven days after admission. On day seven, he developed a remittent fever with an elevation of the soluble interleukin-2 receptor (sIL-2R) level (Table 1, 12 days after admission). This led us to investigate the cerebrospinal fluid (CSF) for possible malignant lymphoma in the central nervous system (CNS). No abnormal findings, including sIL-2R level or malignant cells on cytology, were evident. Therefore, based on the alternative diagnosis of idiopathic transverse myelitis, the treatment for infarction was discontinued, and methylprednisolone (mPSL) pulse therapy (1,000 mg/day for three days) was administered. This did not improve the paraplegia or MRI findings on T2WI. These clinicoradiological inefficacies of the steroid treatment prompted us to perform further examinations to detect any malignancies, including malignant lymphomas. Whole-body contrast-enhanced computer tomography, whole-body gallium scintigraphy, and aspiration and biopsy of the bone marrow were completed; however, no supportive evidence was found. On day 16, a positive fecal occult blood test was obtained; the subsequent colonoscopy showed no malignancy, and the esophagogastroduodenoscopy (EGD) was suggestive of severe atrophic gastritis. On biopsy, an edematous mucosa seen in the gastric fornix had been infiltrated by small to medium-sized slightly atypical lymphoid cells within the lamina propria. Immunohistochemical staining demonstrated CD20(+), CD79a(+), Bcl2(+), CD3(-), CD5(-), and CD10(-). The Ki-67 labeling index was over 50%, despite the low morphological malignancy (data not shown). A pathological diagnosis of gastric extra-nodal marginal zone lymphoma of mucosa-associated lymphoid tissue type (MALT lymphoma) was thus made. The patient received *H. pylori* eradication therapy after a positive urea breath test on day 34. Sixty days after admission, he developed cardiopulmonary arrest due to bleeding from the mucosal lesion in his stomach. A second gastric biopsy was performed, which revealed progression to diffuse large B-cell lymphoma (DLBCL) (Fig. 2). He was successfully resuscitated, but was unable to receive chemotherapy for DLBCL due to his critical status. He died 77 days after admission and an autopsy was performed (Fig. 3).

Autopsy findings

Macroscopically, the spinal cord showed bilateral multifocal softened lesions with hemorrhaging mainly in the gray matter of the spinal cord extending from T3 to S3 segments apparent at the thoracic level (Fig. 4a). Microscopically, these lesions seemed to have been caused by two distinct

Table 1. Laboratory Data on Admission and 12 Days after Admission.

On admission				12 days after admission	
Hematology		**Biochemistry**			
WBC (4-9×10^3/μL)	4.940	TP (6.5-8.3 g/dL)	6.7		
Differential count*1		ALB (3.9-4.9 g/dL)	3.3	ALB	2.0
Neutrophils (42-74%)	61.0	AST (8-38 U/L)	36	AST	47
Eosinophils (0-7%)	1.0	ALT (4-43 U/L)	22	ALT	41
Basophils (0-2%)	0.0	LDH (106-211 U/L)	299	LDH	162
Monocytes (1-8%)	12.0	ALP (103-335 U/L)	200	ALP	186
Lymphocytes (18-50%)	26.0	γGTP (13-66 U/L)	15		
RBC (431-565×10^4/μL)	494	T-bil (0.2-1.2 mg/dL)	1.1	T-bil	0.6
Hb (13.7-17.4 g/dL)	11.1	CK (61-225 U/L)	80		
Ht (40.2-51.5%)	33.3	BUN (9-23 mg/dL)	17.7	BUN	13.7
MCV (83-101 fL)	95.2	Cre (0.6-1.1 mg/dL)	0.41	Cre	0.56
MCH (28.1-34.5 pg)	31.7	UA (3-7 mg/dL)	3.6		
MCHC (31.9-34.7 g/dL)	33.3	CRP (<0.1 mg/dL)	5.43		
Plt (13-38×10^4/uL)	3.9	Anti-AQP4 antibody*2	(-)	β2MG (0.9-2.0 mg/dL)	2.3
		Anti-MOG antibody*3	(-)	sIL-2R (122-496 U/mL)	7,901

The range of normal values are given in parenthesis.

WBC: white blood cell, RBC: red blood cell, Hb: hemoglobin, Ht: hematocrit, MCV: mean corpusclular volume, MCH: mean corpusclular hemoglobin, MCHC: mean corpuscular hemoglobin concentration, Plt: platelet, TP: total protein, ALB: albumin, AST: aspartate aminotransferase, ALT: alanine aminotransferase, LDH: lactate dehydrogenase, ALP: alkaline phosphatase, γGTP: gamma-glutamyltransferase, T-bil: total bilirubin, CK: creatine kinase, BUN: blood urea nitrogen, Cre: creatinine, CRP: C-reactive protein, AQP4: aquaporin4, MOG: myelin-oligodendrocyte glycoprotein, β2MG: β2 micro globulin, sIL-2R: soluble interleukin 2 receptor

*1 Leukocyte differential count was based on visual inspection. All of neutrophils were segmented neutrophils.

*2 anti-AQP4 antibody was measured by enzyme-linked immunosorbent assay (ELISA) and cell-based assay.

*3 anti-MOG antibody was measured by cell-based assay.

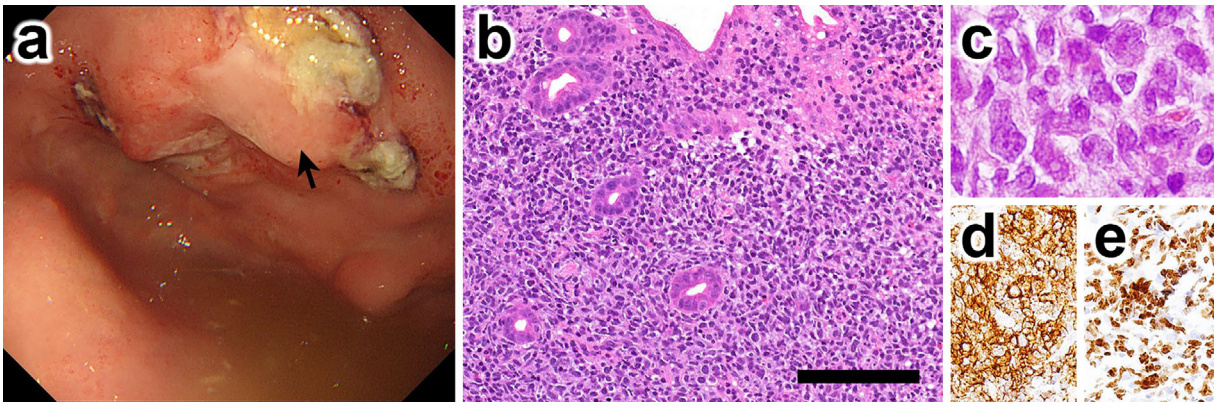

Figure 2. The endoscopic findings and gastric mucosa biopsy findings. a: Esophagogastroduodenoscopy 67 days after admission reveals the growth of the edematous mucosal lesion (arrow). b: The tumor cells with increasing size and cellularity with a high nuclear-to-cytoplasmic ratio [Hematoxylin and Eosin (H&E) staining, ×10]. c: Evident nuclear atypia (H&E staining, ×40). d: The tumor cells with CD20-immunoreactivity (CD20, ×20). e: Ki-67 labeling index over 50% (Ki-67, ×20). Scale bar: 100 μm in b.

disorders: arteriogenic infarction and venous congestion (Table 2). Regarding the arteriogenic infarction, focal necrosis with infiltration of macrophages was observed on the left side of the lateral column at levels T3 to T5 (Fig. 4b-i) and on the right side of the posterior horn from L4 to S1. In contrast to the focal necrosis, severe venous congestion induced extensive necrosis independently of the blood circulation at T6 to T7 (diffuse necrosis) (Fig. 4b-iv) (Table 2). Furthermore, the gray matter hemorrhage (Fig. 4b-ii) and vacuolated changes in the peripheral area of the white matter (peripheral vacuolation) (Fig. 4b-iii) were associated with venous congestion, both of which presented as long cord lesions (Table 2). Some atypical B-lymphocytes were found within the vessel lumens in the CNS, mainly in the venous lumens (Fig. 4c, d) in the spinal cord, whereas no tumor mass was observed in the parenchyma in these areas. Inter-

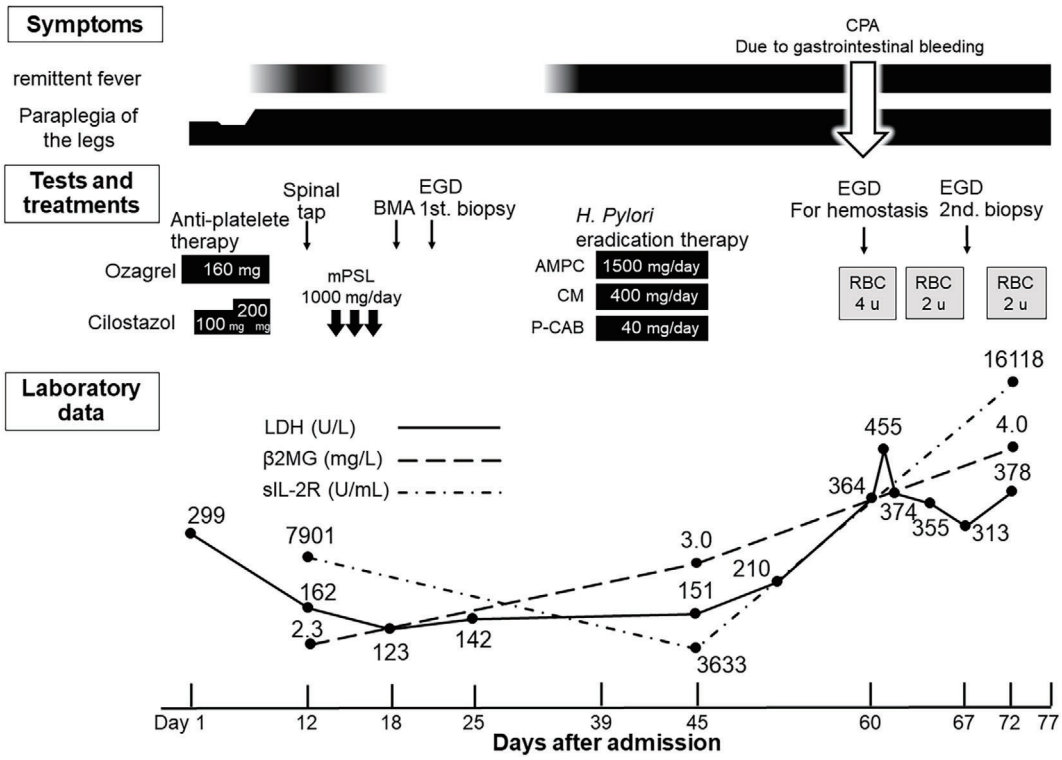

Figure 3. **A summary of the patient's clinical course. The patient died 77 days after admission, approximately 3 months after onset. AMPC: amoxicillin, BMA: bone marrow aspiration, CM: clarithromycin, CPA: cardiopulmonary arrest, EGD: esophagogastroduodenoscopy, LDH: lactate dehydrogenase, mPSL: methylprednisolone, P-CAB: vonoprazan, RBC: red blood cell, sIL-2R: soluble interleukin-2 receptor, u: unit, β2MG: β2-microglobulin**

estingly, tumor cells within the spinal and cerebral vessels and those in the stomach shared some pathological features, such as being medium-sized and showing less morphological malignancy, unlike the common appearance of diffuse B-cell lymphoma. The venous walls in the subarachnoid space and parenchyma adjacent to the lesion presented with fibrous thickening and hyalinization with leakage of the plasma components, some of which were obstructed (Fig. 4e), thus implying subchronic hemodynamic stress under the venous system within the spinal canal. There was no evidence of spinal arteriovenous fistula, which is known to form long spinal cord lesions. A general autopsy revealed metastatic lesions in the liver and spleen. These findings suggested that this patient had experienced a spinal cord infarction and venous congestive myelopathy associated with intravascular large B-cell lymphoma, with the primary lesion originating from the stomach.

Discussion

We experienced a patient with IVLBCL in whom long spinal cord lesions were demonstrated by spinal MRI. Furthermore, we were able to pathologically demonstrate the presence of venous congestion and diffuse necrosis in the intramedullary lesion, suggesting that the long spinal cord lesions had been caused by venous congestive myelopathy associated with IVLBCL.

It may be challenging to clinically establish a diagnosis of IVLBCL and myelopathy due to its rarity. So far, only 6 IVLBCL cases with long spinal cord lesions extending over three or more vertebral segments have been reported (Table 3) (3-8). The clinical presentation in the present case resembled that in the previously reported cases, all of which demonstrated subacute disease onset and primary progression of a motor and sensory deficit, accompanied by longitudinal lesions on spinal MRI (Table 3) (3-8). In three of the six previous cases, immune-mediated disease was suspected. As neuromyelitis optica spectrum disorders (NMOSDs) account for the majority of long spinal cord lesions associated with immune-mediated disease (9, 10), it is important to distinguish NMO from other diseases, including malignant lymphoma, as the cause of long spinal cord lesions. Among the patients with IVLBCL, the reported symptoms differed. On this basis, we propose two features that may be useful for differentiating NMOSDs from IVLBCL: (i) Patients with NMOSDs are relatively younger at disease onset than patients with IVLBCL [40.1±16.3 (11), and 63.9±18.1 years old (Table 3), respectively]. (ii) Patients with NMOSDs show more acute changes in the disease course than patients with IVLBCL. In addition, in NMOSDs, the spinal cord lesions are fully developed at onset and only rarely progress thereafter.

On the other hand, as steroid treatment is generally known to be effective to some extent in both diseases, the

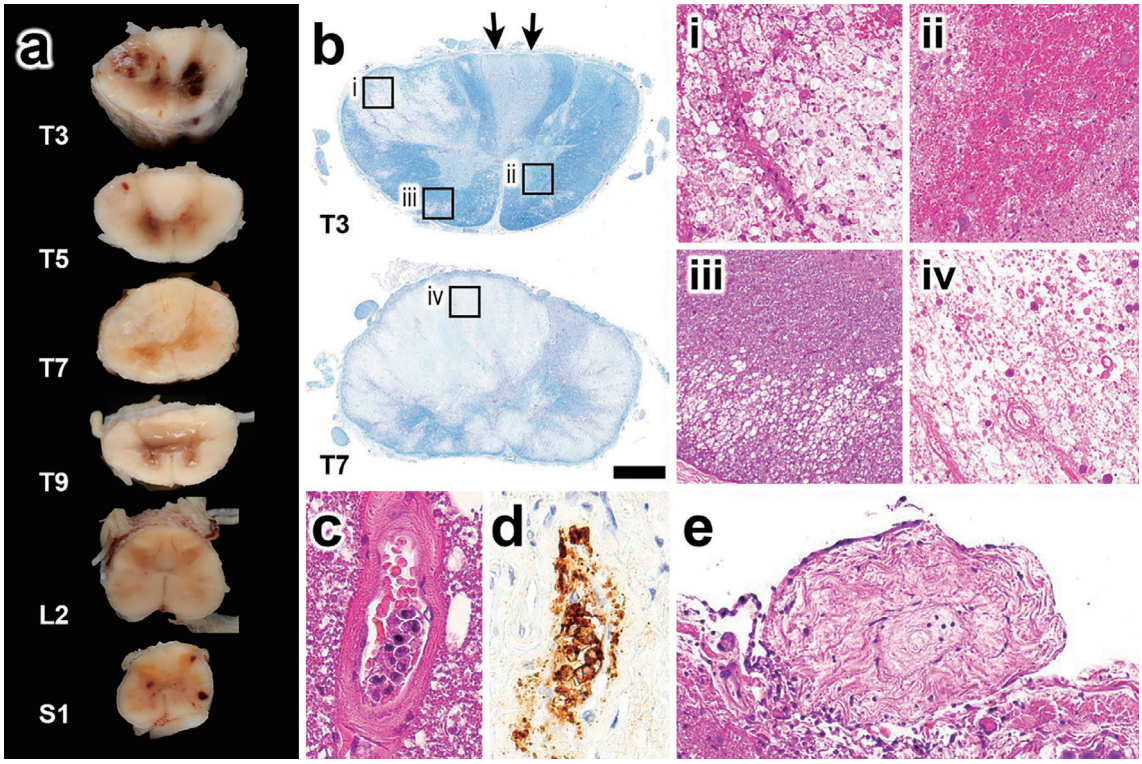

Figure 4. **Histopathologic features of the spinal cord in the studied patient. a: Fixed sections showing extensive and multifocal lesions with hemorrhage from T3 to S1 segments. Note severely affected lesions of the thoracic cord. Macroscopically, no hemorrhagic lesion appears above the level of T2. b: Semi macroscopic features subjected to Klüver-Barrera (KB) staining. Focal lesion of the left lateral column and Wallerian degeneration of the bilateral gracile fasciculus (arrows) in T3. Multifocal lesions in the gray and white matter in T6. i: Focal necrosis, ii: Gray matter hemorrhage, iii: Peripheral vacuolation, iv: Diffuse necrosis [KB, ×1.25, i-iv, Hematoxylin and Eosin (H&E) staining, ×10]. c, d: Some CD20-positive atypical B-lymphocytes within the lumen of the spinal intramedullary vein (c: H&E staining, ×20, d: CD20, ×20). e: A vein in the subarachnoid space with fibrous thickening and obstruction (H&E staining, ×10). Scale bar: 4 mm in a, 1.5 mm in b, 100 μm in i–iv, 25 μm in c and d; 50 μm in e.**

Table 2. **Pathological Findings of the Spinal Cord in the Studied Patient.**

	Arteriogenic feature	Venousgenic features		
Level*	Focal necrosis	Diffuse necrosis	Gray matter hemorrhages	Peripheral vacuolation
C7	-	-	-	++
T3	+; lt. Lateral column	-	+++	+++
T4	+; lt. Lateral column	-	+++	+++
T5	+; lt. Lateral column	-	+++	+++
T6	-	+	Not available**	+++
T7	-	+	Not available**	+++
T9	-	-	+++	++
T10	-	-	+++	++
L2	-	-	+	+
L3	-	-	++	++
L4	+rt. Posterior horn	-	++	+++
S1	+rt. Posterior horn	-	++	++
S2	-	-	+	++
S3	-	-	+	++

The presence or absence of focal necrosis and diffuse necrosis was expressed as "+" or "-", respectively.

The severity of gray matter hemorrhages and peripheral vacuolation were graded according to the semiquantitative evaluation: none:-, mild:+, moderate:++, severe:+++.

* Spinal cord level, microscopically examined,

** Gray matter was not available due to severe destruction caused by diffuse necrosis.

Table 3. **Clinicopathological Features of Reported Cases of Intravascular Lymphoma Presenting Long Spinal Cord Lesions *1.**

Case no.	Reference	Age (years)/ sex	Symptoms	Lesion / length (no. of vertebral bodies)	Clinical diagnosis	Disease course	Serum LDH initial / max (U/L)	Serum sIL-2R initial (U/mL)	Treatments (efficacy)	Time from onset to diagnosis of IVLBCL (months)	Overall survival (months)	Definite diagnostic method	Possible etiology of myelopathy/ pathologic finding
1	(3)	41/M	Conus medullaris syndrome	Conus medullaris/ 3	Acute inflammatory demyelinating disease	Subacute	→ / ND	ND	mPSL (-)*2 CPA (±)*3	13	13	Autopsy	Infarct
2	(4)	52/M	Paraplegia, urinary incontinence	T-L/>9	Asian variant of IVLBCL	Subacute	325 / 737	13,700	R-CHOP (+)	4	Over 42	Muscle, nasal polyps and bone marrow biopsy	ND
3	(5)	82/F	Lower limbs weakness, numbness	T/ 7	Transverse myelitis	Subacute	→ / 488	ND	mPSL (-), PE (-)	14	14	Autopsy	Congestion
4	(6)	45/M	Lower limbs dysesthesia, paraplegia	T-L/ 17	Immune-mediated myelopathy / IVLBCL	Subacute	283 / ND	2,666	mPSL (-) PE (-) R-CHOP (+)	14	Over 26	Renal biopsy	Infarct, immune-mediated (demyelination)
5	(7)	64/F	Lower limbs paraplegia, sensory disturbance	T/ 8	IVLBCL	Subacute	382 / ND	1,670	mPSL (-) R-CHOP (+)	4.5	Over 5	Random skin biopsy	ND
6	(8)	82/F	Paraplegia	C-T/ 11	Myelopathy, intracranial hemorrhages / IVLBCL	Subacute	ND / ND	ND	ND	ND	ND	Random skin biopsy	ND
7	Present case	81/M	Lower limbs paraplegia, sensory disturbance, urinary retention	C-T/ 10	Infarction, Transverse myelitis	Subacute	299*4/ 455	7,901	anti-platelet (-), mPSL (-),	3	3	Autopsy	Infarct, venous congestion

*1 Long spinal cord lesions are defined as 3 or more vertebral segment longitudinally lesions.

*2 The cerebrospinal fluid results improved but the symptoms remained unchanged.

*3 Clinical symptoms as well as CSF parameters and radiologic findings improved slightly.

*4 Decreased to the normal range before mPSL treatment

→: documented as normal range, (+): effective, (-): ineffective, C: cervical, CPA: cyclophosphamide, F: Female, IVLBCL: intravascular large B-cell lymphoma, L: lumbar, M: Male, mPSL: methylprednisolone, ND: Not documented, PE: plasma exchange, R-CHOP: Treatment with rituximab, cyclophosphamide, doxorubicin, vincristine, and prednisone, T: thoracic

efficacy of steroids is not useful for distinguishing the two diseases. However, as was seen in the present case, steroid therapy was not very effective in all four of the previously reported patients who received it (3-8) (Table 3). This may be due to the fact that irreversible vascular-related lesions frequently develop in the spinal cord of patients with IVLBCL (3, 5, 12, 13), meaning that efficacy and functional outcome would depend on the size of the stroke lesion in each case. Therefore, to improve the functional prognosis, IVLBCL needs to be identified early before the lesion ex-

pands.

Elevated levels of LDH and sIL-2R, which are frequently observed in IVLBCL (1), might be helpful indicators of the possible presence of IVLBCL. The level of sIL-2R was elevated in three of the previous cases and the present case (Table 3). On the other hand, in four of the reported cases, the LDH level was initially within the normal range or only slightly elevated (Table 3), thus delaying a definitive diagnosis. Although it has been reported that LDH is a more sensitive indicator than sIL-2R in intravascular malignant lymphoma (14), it may not be applicable to IVL cases with long spinal cord lesions. Indeed, in our patient, LDH decreased to the normal range before mPSL infusion therapy (Fig. 4). This suggests that, in this situation, a thorough and careful systemic examination should be repeated, even if the first examination shows no obvious evidence of malignancy.

Postmortem histopathology in the present case showed that the tumor cells in the gastric mucosal lesions and lymphoma cells in the spinal vessels shared common morphologic features, although the former appeared to be much less malignant. This suggested that a highly proliferative B-cell lymphoma originating in the gastric submucosa had metastasized into the blood vessels and progressed to IVLBCL, while few cases of MALT lymphoma associated with IVLBCL have been reported (15, 16). Although random skin biopsies have been reported to have about 80% sensitivity for a definitive diagnosis of IVLBCL (17), we did not perform it here because of the rapid malignant progression of the gastric mucosal lesion within a few months, and the outcome was distinctly worse than described in the other cases (Table 3). These features appear to reflect the fact that DLBCL that transforms from MALT lymphoma can behave more aggressively than primary DLBCL (15, 18).

Regarding the etiology of the spinal cord lesions in the present case, the focal necrosis and long extensive lesions seemed to be related to the arterial infarct and venous congestion, respectively (Fig. 3) (Table 2). A comparison of the spinal MRI findings with the histopathological findings suggested that the gadolinium enhancement represented the T6 to T7 necrotic lesion, and that the T2WI hyperintensity extending above and below this enhanced area represented venous congestion (Fig. 1, 3) (Table 3). In rare cases, it has been suggested that the azygous vein and vertebral venous plexus may act as a pathway of metastatic spread from abdominal organs to the corpus vertebra and subarachnoid space (19). Similarly, we suspected that in the present case the lymphoma cells from the stomach had involved these veins, thereby increasing the intramedullary venous pressure in the spinal cord, and thus leading to the onset of arterial infarct. As a result, the venous congestion may have worsened and caused the progressive long cord lesions. This speculation is consistent with the disease course.

In conclusion, IVLBCL is rarely associated with long spinal cord lesions due to venous congestion. If elderly patients show symptoms related to subacute myelopathy and spinal MRI demonstrates expanding long spinal cord lesions, then further examinations such as serum sIL-2R and skin biopsy are needed in order to make an unequivocal diagnosis of IVLBCL.

The authors state that they have no Conflict of Interest (COI).

Acknowledgement

We are grateful to the patient and his family for acceptance of the postmortem examination. We would like to thank Dr. Keiko Tanaka for measuring the anti-AQP4 antibody and the anti-MOG antibody using cell-based assays and for her valuable opinions on the diagnosis of this case.

References

1. Sukswai N, Lyapichev K, Khoury JD, Medeiros LJ. Diffuse large B-cell lymphoma variants: an update. Pathology **52**: 53-67, 2020.
2. Shimada K, Murase T, Matsue K, et al. Central nervous system involvement in intravascular large B-cell lymphoma: a retrospective analysis of 109 patients. Cancer Sci **101**: 1480-1486, 2010.
3. Schwarz S, Zoubaa S, Knauth M, Sommer C, Storch-Hagenlocher B. Intravascular lymphomatosis presenting with a conus medullaris syndrome mimicking disseminated encephalomyelitis. Neuro Oncol **4**: 187-191, 2002.
4. Takizawa S, Shirasugi Y, Nakamura N, et al. An atypical form of Asian variant of intravascular large B-cell lymphoma presenting with myelopathy alone for 4 months prior to pancytopenia. Intern Med **46**: 1879-1880, 2007.
5. Kumar N, Keegan BM, Rodriguez FJ, Hammack JE, Kantarci OH. Intravascular lymphoma presenting as a longitudinally-extensive myelitis: diagnostic challenges and etiologic clues. J Neurol Sci **303**: 146-149, 2011.
6. Shirai S, Takahashi I, Kanoh T, et al. [A case of intravascular lymphoma with a longitudinal spinal lesion diagnosed by multiple biopsies]. Rinsho Shinkeigaku (Clin Neurol) **52**: 336-343, 2012.
7. Yamazaki H, Imai K, Hamanaka M, et al. [A case of acute progressive myelopathy due to intravascular large B cell lymphoma diagnosed with only random skin biopsy]. Rinsho Shinkeigaku (Clin Neurol) **55**: 115-118, 2015.
8. Orimo K, Sasaki T, Kakuta Y, Imafuku I. Intravascular lymphoma presenting as myelopathy and intracranial hemorrhages. Intern Med **59**: 3249, 2020.
9. Trebst C, Raab P, Voss EV, et al. Longitudinal extensive transverse myelitis - it's not all neuromyelitis optica. Nat Rev Neurol **7**: 688-698, 2011.
10. Jain RS, Kumar S, Mathur T, Tejwani S. Longitudinally extensive transverse myelitis: A retrospective analysis of sixty-four patients at tertiary care center of North-West India. Clin Neurol Neurosurg **148**: 5-12, 2016.
11. Ghezzi A, Bergamaschi R, Martinelli V, et al. Clinical characteristics, course and prognosis of relapsing Devic's Neuromyelitis Optica. J Neurol **251**: 47-52, 2004.
12. Liu H, Koyanagi I, Chiba H, et al. Spinal cord infarct as the initial clinical presentation of intravascular malignant lymphomatosis. J Clin Neurosci **16**: 570-573, 2009.
13. Lyden S, Dafer RM. Intravascular lymphomatosis presenting with spinal cord infarction and recurrent ischemic strokes. J Stroke Cerebrovasc Dis **28**: e132-e134, 2019.
14. Shimada K, Matsue K, Yamamoto K, et al. Retrospective analysis of intravascular large B-cell lymphoma treated with rituximab-containing chemotherapy as reported by the IVL study group in Japan. J Clin Oncol **26**: 3189-3195, 2008.
15. Ghesquières H, Berger F, Felman P, et al. Clinicopathologic characteristics and outcome of diffuse large B-cell lymphomas presenting with an associated low-grade component at diagnosis. J Clin

Oncol **24**: 5234-5241, 2006.

16. Matysiak-Budnik T, Jamet P, Ruskoné-Fourmestraux A, et al. Gastric MALT lymphoma in a population-based study in France: clinical features, treatments and survival. Aliment Pharmacol Ther **50**: 654-663, 2019.

17. Matsue K, Abe Y, Kitadate A, et al. Sensitivity and specificity of incisional random skin biopsy for diagnosis of intravascular large B-cell lymphoma. Blood **133**: 1257-1259, 2019.

18. Hashmi AA, Hussain ZF, Faridi N, Khurshid A. Distribution of Ki 67 proliferative indices among WHO subtypes of non-Hodgkin's lymphoma: association with other clinical parameters. Asian Pac J Cancer Prev **15**: 8759-8763, 2014.

19. Lee JL, Kang YK, Kim TW, et al. Leptomeningeal carcinomatosis in gastric cancer. J Neurooncol **66**: 167-174, 2004.